Journal of Alloys and Compounds 513 (2012) 445–448

Contents lists available at SciVerse ScienceDirect

Journal of Alloys and Compounds

journal homepage: www.elsevier.com/locate/jallcom

# The effects of Ni–Na codoping on structure and properties of ZnO films by pulsed laser deposition

Jie Jiang[a], Xuetao Wang[a], Liping Zhu[a,*], Yinzhu Zhang[a], Zhizhen Ye[a], Bo He[b]

[a] State Key Laboratory of Silicon Materials, Department of Materials Science and Engineering, Zhejiang University, Hangzhou 310027, People's Republic of China
[b] National Synchrotron Radiation Laboratory, University of Science and Technology of China, Hefei 230029, People's Republic of China

ARTICLE INFO

*Article history:*
Received 8 September 2011
Received in revised form 19 October 2011
Accepted 19 October 2011
Available online 7 November 2011

*Keywords:*
Room-temperature ferromagnetism
p-Type
Ni–Na codoped ZnO film
Pulsed laser deposition

ABSTRACT

The Ni-doped and Ni–Na codoped ZnO thin films have been prepared on quartz substrates by pulsed laser deposition. The effect of Na on the magnetic and electrical properties of Ni-doped ZnO has been investigated. The dopant $Na^+$ was identified by XPS measurement. The Hall measurement showed weak p-type property in the Ni–Na codoped ZnO thin film. The room-temperature ferromagnetism in the Ni–Na codoped ZnO thin film was obviously enhanced due to the strengthening of the ferromagnetic exchange interaction by the p-type dopant $Na^+$. The possible fabrication of ZnO-based p-type diluted magnetic semiconductors should be of interest for spintronic applications.



## 1. Introduction

ZnO is a compound semiconductor with a wide direct band gap of 3.37 eV and a large exciton binding energy of 60 meV at room temperature, which is an attractive candidate for a variety of device applications [1,2]. Recently, ZnO-based diluted magnetic semiconductors (DMSs) doped with transition metal (TM) have been extensively investigated both in theory [3,4] and experiments [5,6] for their potential applications in spin electronics through the utilization of both electron charge and spin degree of freedom [7]. Initially Dietl et al. [4] predicted theoretically that room-temperature ferromagnetism can be achieved in p-type doped ZnO. Also, series of theoretical analysis indicated that the room-temperature ferromagnetism could strongly be promoted by p-type doping in ZnO [8]. Since the presence of additional carriers plays an important role in stabilizing or enhancing the magnetic couplings by the codoping ions, the mechanism of room-temperature ferromagnetism is still in debate. Sluiter et al. [9] and Gu et al. [10] experimentally showed that the Li or Na codoping in the Co-doped ZnO as p-type carriers amplifies the magnetic couplings. Wang et al. [11] studied N-codoped ZnO:Mn thin films and predicted that N codoping generally enhances the stability of a ferromagnetism state over an antiferromagnetic state. Wan [12] experimentally reported that p-type conduction is necessary for the observation of ferromagnetism in Mn–P codoped ZnO films at room temperature. However, Sato and Katayama-Yoshida [13] predicted that room-temperature ferromagnetism in Co-doped ZnO could be due to n-type carriers by using the first-principles calculations. When compared with the Co or Mn doped ZnO thin films, relatively few studies [14,15] have been reported in the Ni-doped ZnO system since its preparation is particularly challenging due to the large driving force for phase segregation into NiO and ZnO [16]. In this paper, PLD was used to deposit Ni-doped ZnO films, so as to enhance Ni solid solubility in ZnO films without second phases. In particular, we hardly find any experimental report on the room-temperature ferromagnetism studies in Ni–Na codoped ZnO thin films. Theoretically, group-I impurities, such as Li and Na, have a relative shallower acceptor level in ZnO [17]. In previous research, our group has demonstrated that Na could be an effective dopant for realizing p-type conductivity in ZnO [18]. As Na locates in group-I and without its own 3d electrons to interfere with magnetic ordering, we can study the influence of the carriers or $Na^+$ ions on the room-temperature ferromagnetism. Hence, in this work, we have prepared the p-type Ni–Na codoped ZnO thin film by PLD and made effort to carry out electrical and magnetic studies to understand the origin of ferromagnetism, if any, in ZnO.

## 2. Experimental details

Ni-doped, Ni–Na codoped ZnO thin films (ZnNiO, Zn(Ni,Na)O) were deposited on quartz substrates by pulsed laser deposition (PLD). The ceramic targets were prepared by mixing ZnO (99.99%), Ni (99.99%) and $Na_2CO_3$ (99.99%) powders. The Ni content is 3 at.% in the ZnNiO target, and the Ni and Na content are 3 at.% and 1 at.% in the Zn(Ni,Na)O target, respectively. The working pressure in the chamber was 10 Pa with $O_2$ as the ambient gas. A KrF excimer laser (Compex102, 248 nm,

* Corresponding author. Tel.: +86 571 87953139; fax: +86 571 87952625.
*E-mail addresses:* zlp1@zju.cdu.cn, zjuzlp@163.com (L. Zhu).

0925-8388/$ – see front matter © 2011 Published by Elsevier B.V.
doi:10.1016/j.jallcom.2011.10.074

25 ns) was used as the ablation source. The substrates were held at 500 °C during the film deposition.

The crystallographic structure of the samples was investigated by the Bede D1 X-ray diffraction (XRD) system with Cu Kα radiation (λ = 0.15406 nm). The chemical states of the elements present in the samples and the element contains were identified by the X-ray photoelectron spectroscopy (XPS). The electrical properties were measured by using a four-point probe van der Pauw configuration (HL5500PC) at room temperature. Ni K-edge X-ray absorption near-edge structure (XANES) was used to determine the valence state and local geometry of the Ni dopant in the ZnO lattice. The magnetic properties were measured by a superconducting quantum interference device (SQUID) magnetometer.

## 3. Results and discussion

Fig. 1 shows the XRD pattern of Zn(Ni,Na)O thin film and that of ZnNiO film for comparison. Only (0 0 2) peaks around 34° were observed in both samples, demonstrating that a high c-axis preferential orientation and single-phase wurtzite of the deposited films. There were no other phases such as nickel oxide or metal nickel up to the instrument's detection limit. It is also noted that the intensity of the (0 0 2) peak in the Zn(Ni,Na)O film reduces, indicating degraded crystallinity caused by Na doping. The inset of Fig. 1 shows the particular position of peaks. Theoretically, since the ion radius of $Ni^{2+}$ (0.72 Å) is close to and smaller than that of $Zn^{2+}$ (0.74 Å), with the assumption that all the dopant Ni would substitute for Zn, the (0 0 2) peak of ZnNiO film should move to larger angle slightly or stay at the same angle when compared to that of a pure ZnO film ($2\theta = 34.43°$) obtained at the same condition. From the inset of Fig. 1, we see that our experimental results are in accord with the theory, confirming the doping behavior of Ni. We can also find that the peak of the Zn(Ni,Na)O film shift to lower angle when compared to that of the ZnNiO film. Noting that the ion radius of $Na^+$ is 1.02 Å, which is larger than that of $Zn^{2+}$ (0.74 Å); substituting Na for Zn will induce the expansion of the ZnO lattice and cause the lower angle shifting of the (0 0 2) peak [18]. The grain size is calculated by Scherer expressions: $D = 0.89\lambda/\beta \cos\theta$, where $D$ denotes the diameter along $c$-axis, $\lambda$ is the wavelength of X-ray ($\lambda = 0.15406$ nm), $\beta$ is the full width at half maximum (FWHM) and $\theta$ is the half diffraction angle. By calculation we get the results that the ZnNiO and Zn(Ni,Na)O films have the grain size of 31.56 nm and 31.77 nm, respectively. The presence of grain boundaries and grain boundary segregation increases the overall solubility of dopants without appearance of a second phase [19,20].

The chemical states of the elements present are discussed according to the XPS measurements. The substitution of Ni ions was confirmed by Ni 2p XPS spectrum shown in Fig. 2(b). The Ni $2p_{3/2}$ peaks occur at 855.87 eV and 855.64 eV, while Ni $2p_{1/2}$ peaks locate at 873.48 eV and 873.21 eV, respectively for the ZnNiO and Zn(Ni,Na)O films. The Ni $2p_{3/2}$ peak position was close to the value of NiO, while quite different from that of Ni and $Ni_2O_3$, indicating $Ni^{2+}$ in the ZnNiO and Zn(Ni,Na)O films [21,22]. We did not find any double peak structures in the $2p_{3/2}$ peak of our samples, suggesting the absence of NiO [23]. Besides, the energy difference between the Ni $2p_{3/2}$ and $2p_{1/2}$ peaks is about 17.6 eV, which is strikingly different from that of NiO (18.4 eV) [24]. The above results strongly suggest that Ni atoms were successfully incorporated into ZnO without forming any other phases. We employed Ni K-edge XANES to confirm the valence state and local geometry of the Ni dopant further.

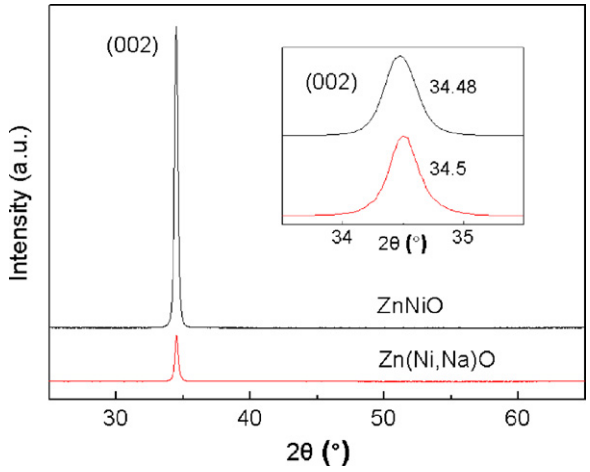


**Fig. 1.** XRD patterns of ZnNiO and Zn(Ni,Na)O films.

In order to confirm the environment of Ni and Na, the Zn 2p and O 1s core level spectra were given in Fig. 2(a) and 2(c), respectively. It is noted that the Zn $2p_{3/2}$ peak of the Zn(Ni,Na)O film moved to lower energy compared to that of the ZnNiO film. Since the same phenomenon was found in the O 1s peaks, it was not accidental. We believe that the dopant Na substituted for the Zn site of the lattice forming $Na^+$–$O^{2-}$–$Zn^{2+}$ and the binding energy of the Zn 2p and O 1s decrease owning to the lower electronegativity of Na. The absorption peaks of O 1s can be divided into two nearly Gaussian peaks, which centered at 530.3 eV and 531.6 eV for the ZnNiO film and centered at 530.13 eV and 531.17 eV for the Zn(Ni,Na)O film. According to the data on the spectra of other related studies, the peaks on the low binding energy side at 530.3 eV and 530.13 eV could be attributed to $O^{2-}$ ions on the wurtzite structure of the hexagonal $Zn^{2+}$ ion array, surrounded by Zn (or substitution Ni and Na) atoms [25,26]. While the high binding-energy peaks at 531.6 eV and 531.17 eV were associated with $O^{2-}$ ions that were in oxygen-deficient regions within the matrix of ZnO [27]. Fig. 2(d) shows the Na 1s peak centered at 1071.13 eV, which could attributed to $Na^+$ according to the handbook of the X-ray photoelectron spectroscopy.

We employed Ni K-edge XANES spectra in Fig. 3 to confirm the valence state and local geometry of the Ni dopant further. In the Ni K-edge XANES spectrum, the feature Ni metal observed at 8333 eV (approximately) is associated with $Ni^0$ and can be used to determine the presence of Ni metal. Therefore, it is clear that the plateau near threshold ($E_0$) associated with $Ni^0$ is absent in spectra for ZnNiO and Zn(Ni,Na)O as well as in the spectrum of NiO. Thus there is no detectable $Ni^0$ in the ZnNiO and Zn(Ni,Na)O films. Similarly, the obvious difference between the spectra of NiO and ZnNiO (or Zn(Ni,Na)O) indicates that Ni substituted for the Zn site of the lattice instead of the formation of NiO. The XANES spectra of Ni in the ZnNiO and Zn(Ni,Na)O thin films show similar features, referred to, as A (the pre-edge), B (the main edge), C (a multiple scattering resonance). These observed peaks are exactly the replication of the calculated spectrum of $Zn_{0.97}Ni_{0.03}O$ film by using ab initio self-consistent FEFF 8.2 code on Ni K edge referred to Ref. [28]. It also can be found that the dopant Na could not change the Ni state in the ZnNiO film.

Fig. 4 shows the magnetization hysteresis loops of the ZnNiO and Zn(Ni,Na)O films at room temperature. The magnetic field was applied parallel to the film plane, and the background hysteresis loops were subtracted. Both S-shaped magnetization hysteresis loops indicate room-temperature ferromagnetism. The coercivity (Hc) of the ZnNiO film was around 15 Oe at room temperature, and the saturation magnetization (Ms) was ~0.12 emu/g (~0.06 $\mu_B$/at.). When Na was doped into ZnNiO film, the coercivity increased remarkably to 100 Oe with the saturation magnetization of 0.16 emu/g (~0.08 $\mu_B$/at.) in the Zn(Ni,Na)O film.

The ferromagnetic behavior might be influenced by the grain boundaries [29,30] and texture [31]. However, this factor could not explain the difference between the two samples as both are the same grain sizes and texture. The unambiguous enhancement of the room-temperature ferromagnetism in the Zn(Ni,Na)O film can only be attributed to Na ion rather than any other Ni

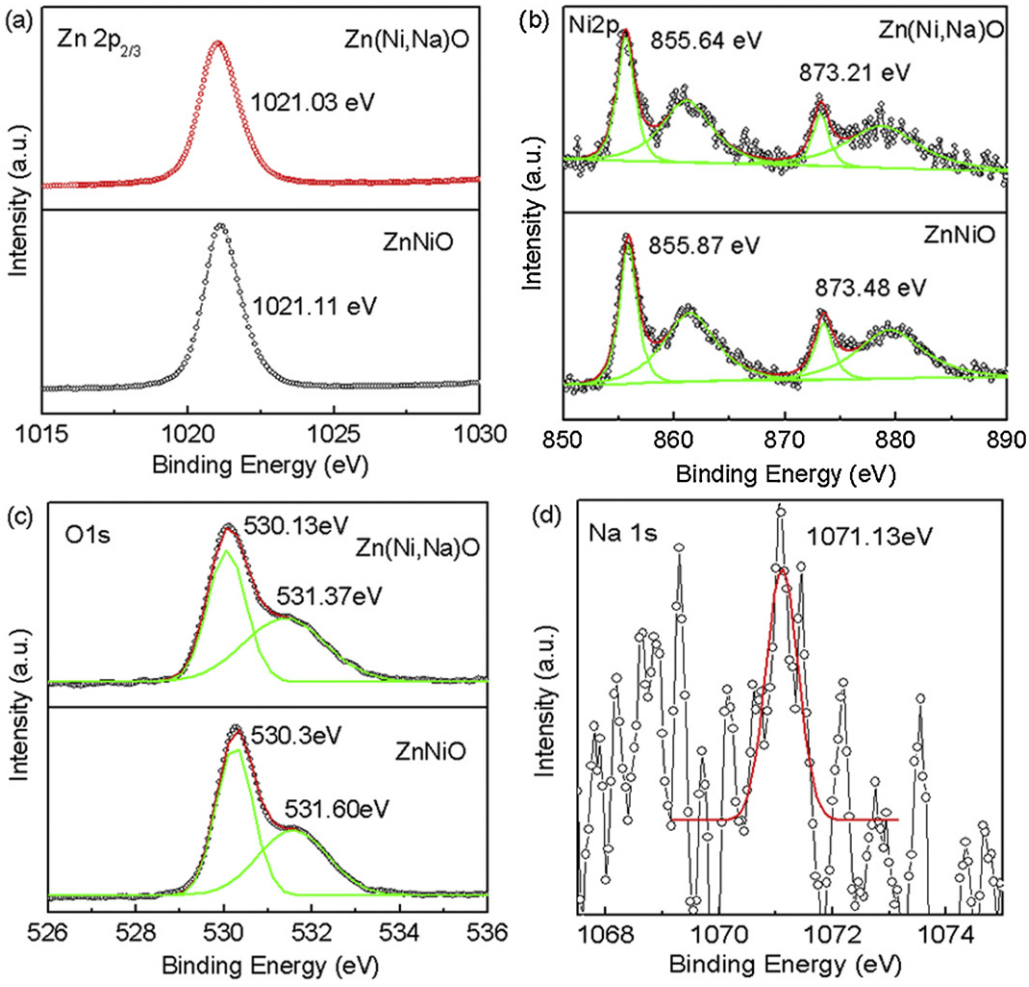


**Fig. 2.** XPS spectra of (a) Zn, (b) Ni, (c) O in ZnNiO and Zn(Ni,Na)O films, and (d) XPS spectra of Na in Zn(Ni,Na)O film.

related phases, which have been ruled out through the XPS and XANES measurements. Based on the widely used carrier-induced ferromagnetic mechanism, a large amount of free carriers is one important factor to get room-temperature ferromagnetism [32]. Carrier concentrations of both samples were characterized by Hall-effect measurement. The results indicate that the ZnNiO film is n-type with the carrier concentration of $6.51 \times 10^{19}$ cm$^{-3}$, the resistivity of 0.0198 Ω cm and the hall mobility of 4.84 cm$^2$ V$^{-1}$ s$^{-1}$. When Na is doped into the ZnNiO film, the film displays weak p-type property with the hole concentration of $4.13 \times 10^{15}$ cm$^{-3}$, the resistivity of 2659 Ω cm and the hall mobility of 0.568 cm$^2$ V$^{-1}$ s$^{-1}$. The remarkable change of the electrical property is surely because of the Na dopant and the enhancement of hole concentration might be caused by the substitution of $Na^+$ for $Zn^{2+}$. It could be indicated that the dopant Na is at the status of deep acceptor level as suggested by Park et al. [17] Considering the high resistivity

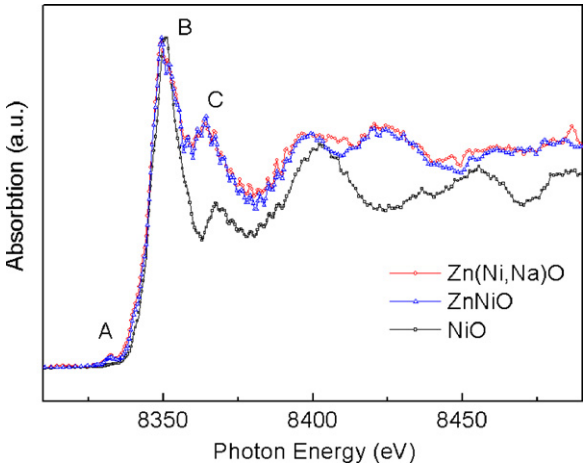


**Fig. 3.** Ni K-edge XANES spectra for various specimens: NiO, ZnNiO, and Zn(Ni,Na)O.

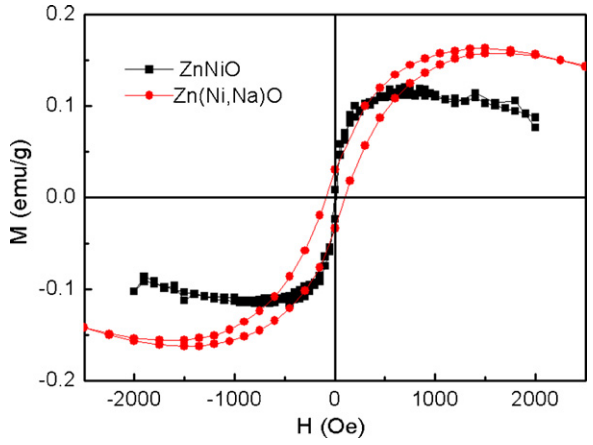


**Fig. 4.** Magnetic loops of the ZnNiO and Zn(Ni,Na)O films measured at room temperature.

of the Zn(Ni,Na)O sample, the traditional RKKY mechanism cannot be applied for the low level itinerant electrons. Ferromagnetic coupling of TM ions via an electron trapped in a bridging oxygen vacancy (F center) was proposed to explain room-temperature ferromagnetism by Coey et al., which can also be applied on our samples [33]. We expect that $Ni^{2+}$–$V_O$–$Ni^{2+}$ groups will be common in the structure. An electron trapped in the oxygen vacancy constitutes an F center, where the electron occupies an orbital which overlaps the d shells of both Ni ions. These F centers are helpful to the ferromagnetic coupling of $Ni^{2+}$. When the p-type Na dopants were doped into the ZnNiO DMS lattice, F centers could be influenced. Our experimental results exhibit a strong predominance of room-temperature ferromagnetism in the Zn(Ni,Na)O sample, indicating that the p-type dopant $Na^+$ might strengthen the effective F center coupling with the magnetic Ni ions in ferromagnetic exchange interaction. Gu et al. [10] also have reported a strong predominance of ferromagnetism at room temperature in the Na doping ZnCoO sample, which was in accordance with our results.

## 4. Conclusion

In summary, the ZnNiO and Zn(Ni,Na)O thin films have been prepared by PLD.

The XRD, XPS and XANFS analyses of both samples suggest that both are single-phase wurtzite structure without any other phases. The weak p-type property has been obtained by Na codoping, which was characterized by Hall-effect measurement. The observed room-temperature ferromagnetism can be attributed to the direct ferromagnetic exchange interaction via electron trapped in a bridging oxygen vacancy coupled with the magnetic Ni ions. The p-type dopant $Na^+$ might strengthen the effective F center mediation in ferromagnetic exchange interaction, leading to the enhancement of the room-temperature ferromagnetism in the Zn(Ni,Na)O sample. By Na and Ni codoping, we may be able to achieve ZnO-based p-type DMSs, which should be important for the development of the ZnO-based spintronic devices.

## Acknowledgements

This work was supported by National Natural Science Foundation of China 51072181 and Doctoral Fund of Ministry of Education of China under Grant No. 20090101110044.

## References

[1] D.C. Look, Mater. Sci. Eng. B 80 (2001) 383.
[2] Z.K. Tang, G.K.L. Wong, P. Yu, M. Kawasaki, A. Ohtomo, H. Koinuma, Y. Segawa, Appl. Phys. Lett. 72 (1998) 3270.
[3] K. Sato, H. Katayama-Yoshida, Jpn. J. Appl. Phys. Part 2 39 (2000) L555.
[4] T. Dietl, H. Ohno, F. Matsukura, J. Cibert, D. Ferrand, Science 287 (2000) 1019.
[5] K. Ueda, H. Tabat, T. Kawai, Appl. Phys. Lett. 79 (2001) 988.
[6] H.J. Lee, S.Y. Jeong, C.R. Cho, C.H. Park, Appl. Phys. Lett. 81 (2002) 4020.
[7] S.A. Wolf, D.D. Awschalom, R.A. Buhrman, J.M. Daughton, S. vonMolnár, M.L. Roukes, A.Y. Chtchelkanova, D.M. Treger, Science 294 (2001) 1488.
[8] N.A. Spaldin, Phys. Rev. B 69 (2004) 125201.
[9] M.H.F. Sluiter, Y. Kawazoe, P. Sharma, A. Inoue, A.R. Raju, C. Rout, U.V. Waghmare, Phys. Rev. Lett. 94 (2005) 187204.
[10] H. Gu, Y.Z. Jiang, Y.B. Xu, M. Yan, Appl. Phys. Lett. 98 (2011) 012502.
[11] Q. Wang, Q. Sun, P. Jena, Y. Kawazoe, Phys. Rev. B 70 (2004) 052408.
[12] Q. Wan, Appl. Phys. Lett. 89 (2006) 082515.
[13] K. Sato, H. Katayama-Yoshida, Semicond. Sci. Technol. 17 (2002) 367.
[14] D.A. Schwartz, K.R. Kittilstved, D.R. Gamelin, Appl. Phys. Lett. 85 (2004) 1395.
[15] P.V. Radovanovic, D.R. Gamelin, Phys. Rev. Lett. 91 (2003) 157202.
[16] V. Jayaram, B.S. Rani, Mater. Sci. Eng. A 304 (2001) 800.
[17] C.H. Park, S.B. Zhang, S.H. Wei, Phys. Rev. B 66 (2002) 073202.
[18] S.S. Lin, Z.Z. Ye, J.G. Lu, H.P. He, L.X. Chen, X.Q. Gu, J.Y. Huang, L.P. Zhu, B.H. Zhao, J. Phys. D: Appl. Phys. 41 (2008) 155114.
[19] B.B. Straumal, A.A. Mazilkin, S.G. Protasova, A.A. Myatiev, P.B. Straumal, B. Baretzky, Acta Mater. 56 (2008) 6246.
[20] B.B. Straumal, B. Baretzky, A.A. Mazilkin, et al., J. Eur. Ceram. Soc. 29 (2009) 1963.
[21] C.D. Wagner, W.M. Riggs, L.E. Davis, J.F. Moulder, Handbook of X-ray Photoelectron Spectroscopy, Perkin Elmer, Eden Prairie, 1979, p. 81.
[22] G.H. Yu, L.R. Zeng, F.W. Zhu, C.L. Chai, W.Y. Lai, J. Appl. Phys. 90 (2001) 4039.
[23] S. Altieri, L.H. Tjeng, A. Tanaka, G.A. Sawatzky, Phys. Rev. B 61 (2000) 13403.
[24] Z.G. Yin, N.F. Chen, F. Yang, S.L. Song, C.L. Chai, J. Zhong, H.J. Qian, K. Ibrahim, Solid State Commun. 135 (2005) 430.
[25] M. Chen, X. Wang, Y.H. Yu, Z.L. Pei, X.D. Bai, C. Sun, R.F. Huang, L.S. Wen, Appl. Surf. Sci. 158 (2000) 134.
[26] L.Q. Zhang, Z.Z. Ye, J.G. Lu, B. Lu, Y.Z. Zhang, L.P. Zhu, J. Zhang, D. Yang, K.W. Wu, J. Huang, Z. Xie, J. Phys. D: Appl. Phys. 43 (2010) 015001.
[27] M. Futsuhara, K. Yoshioka, O. Takai, Thin Solid Films 317 (1998) 322.
[28] J. Iqbal, B.Q. Wang, X.F. Liu, D.P. Yu, B. He, R.H. Yu, New J. Phys. 11 (2009) 063009.
[29] B.B. Straumal, S.G. Protasova, A.A. Mazilkin, A.A. Myatiev, P.B. Straumal, G. Schütz, E. Goering, B. Baretzky, J. Appl. Phys. 108 (2010) 073923.
[30] B.B. Straumal, A.A. Mazilkin, S.G. Protasova, A.A. Myatiev, P.B. Straumal, G. Schütz, P.A. van Aken, E. Goering, B. Baretzky, Phys. Rev. B 79 (2009) 205206.
[31] B. Straumal, A. Mazilkin, S. Protasova, A. Myatiev, P. Straumal, E. Georing, B. Baretzky, Phys. Status Solidi B 248 (2011) 1581.
[32] T. Zhao, S.R. Shinde, S.B. Ogale, H. Zheng, T. Venkatesan, R. Ramesh, S. Das Sarma, Phys. Rev. Lett. 94 (2005) 126601.
[33] J.M.D. Coey, A. Douvalis, C. Fitzgerald, M. Venkatesan, Appl. Phys. Lett. 84 (2004) 1332.